Journal of Zhejiang University-SCIENCE A (Applied Physics & Engineering)
ISSN 1673-565X (Print); ISSN 1862-1775 (Online)
www.zju.edu.cn/jzus; www.springerlink.com
E-mail: jzus@zju.edu.cn

Mechanical behavior of a shelter system based on cable-strut structures*

Jian-guo CAI†[1,2], Ya ZHOU[1], Jian FENG†[1,2], Yi-xiang XU[3]

([1]*Key Laboratory of C&PC Structures of Ministry of Education, Southeast University, Nanjing 210096, China*)

([2]*National Prestress Engineering Research Center, Southeast University, Nanjing 210096, China*)

([3]*Department of Civil Engineering, Strathclyde University, Glasgow, UK*)

†E-mail: {j.cai; fengjian}@seu.edu.cn

Received July 6, 2012; Revision accepted Oct. 30, 2012; Crosschecked Nov. 15, 2012

Abstract: A shelter system based on cable-strut structures, consisting of compressive struts and high-tensile elements, is described in this paper. The deployment of the shelter is achieved by tightening inclined cables. Lower cables are used to terminate the deployment. The state of self-stress of the cable-strut structures in the fully deployed configuration is given, and the minimum strut length and the maximum load design of the shelter are discussed. The mechanical behavior of the system was studied under symmetrical and asymmetrical load cases. The results show that the shelter in the deployed configuration satisfies the ultimate limit and the serviceability limit state conditions. Finally, the stability of the cable-strut system is investigated, considering the effect of imperfections on the buckling of the shelter. We conclude that the influence of imperfections based on the consistent imperfection mode method is not significant.

Key words: Foldable structures, Cable-strut structures, Mechanical behavior, Self-stress, Stability
doi:10.1631/jzus.A1200172 **Document code:** A **CLC number:** TU399

1 Introduction

In recent years, space structures have been developing rapidly all over the world. Cable structures are found in many large space structures (Hosozawa *et al*., 1999; Liu *et al*., 2011). They can be divided into two types: thoroughbred tension structures (Hangai and Wu, 1999; Juan and Mirats Tur, 2008; Luchsinger, *et al.*, 2011) and hybrid tension structures. Hybrid tension structures can also be categorized as (1) structures using members, such as semi-rigid hanging members, which are made by changing the properties of tension members for pure tension structures; (2) structures made by combining tension members with rigid members such as arches, beams, and struts (Saitoh and Okada, 1999; Xue and Liu, 2009).

Tensegrity structures, in which the compressed members (usually bars or struts) do not touch each other and the prestressed tensioned members (usually cables or tendons) delineate the system spatially, were proposed in the middle of the last century (Motro, 2003). Recently, cable-strut structures, in which struts can touch each other, were proposed by Wang (1998) and Wang and Li (2003a; 2003b) and Liew *et al*. (2003). They showed that cable-strut structures are higher in structural efficiency than the conventional double-layer space truss (Makowski, 1981) and tensegrity structures (Motro, 2003). Many types of cable-strut structures and their applications were reviewed by Wang and Li (2003a; 2003b).

The study of deployable structures is an important topic in space structures. Research in deployable structures has focused largely on aerospace

* Project supported by the National Natural Science Foundation of China (No. 51278116), the Jiangsu "Six Top Talent" Program of China (No. 07-F-008), the Priority Academic Program Development of Jiangsu Higher Education Institutions, and the Scientific Research Foundation of Graduate School of Southeast University (No. YBJJ0817), China

applications. However, recent conflicts and natural disasters suggest an increasing need to consider the application of these structures to deployable shelters for both military and humanitarian aid purposes (Melin, 2004). Many deployable structures have been developed based on bar elements and a few based on plate elements (De Temmerman *et al*., 2007; Mao *et al*., 2007; Cai *et al*., 2012; Gioia *et al.*, 2012; Seffen, 2012). In bar systems, the most commonly used deployable structures applied to shelters are realized by scissor elements, which consist of two bars connected by a hinge. They are combined to create shelters with internal mobility. Compared with bar forms, deployable tensegrity systems can achieve a much smaller stowed volume and have a simpler joint design (Motro, 1992). The main folding methods of tensegrity systems are telescoping struts, releasing cables, and the combination of the two methods, as suggested by Motro (2003). This type of structure has been used in double-layer grids and deployable footbridges (Quirant *et al*., 2003; Rhode-Barbarigos *et al*., 2012). Recently, a new type of foldable structure, a deployable cable-strut structure, was proposed (Vu *et al*., 2005; 2006a; 2006b; Liew and Tran, 2006; Li *et al*., 2011). Compared with a bar system, cable-strut grids can achieve a smaller stowed volume and have a reduced number of articulated joints with complicated mechanisms. Compared with tensegrity structures, they may have higher structural efficiency.

This paper introduces the concept of a foldable shelter based on a cable-strut system, which can be deployed quickly on site while maintaining good structural efficiency, and thus can meet the global demand for this type of structural system. The practical design and analysis issues of the domed shelter are discussed in relation to its feasibility in terms of its deployability and kinematic constraints. The linear and nonlinear buckling analyses of the shelter are investigated. The effects of imperfections on structural behavior are also taken into account.

2 Design of the cable-strut system

2.1 Concept design

The proposed system is constructed using compressive struts and high-tensile elements that are connected with pin joints. This structure, which is called a crystal-cell pyramid (CP) (Wang, 1998), can be seen as two pyramids, one on top of the other, attached to each other at the base (Fig. 1). It comprises a vertical strut and inclined struts, and some lower cables and inclined cables. The lower cables surround the base and the inclined cables form the diagonal edges of the structure.

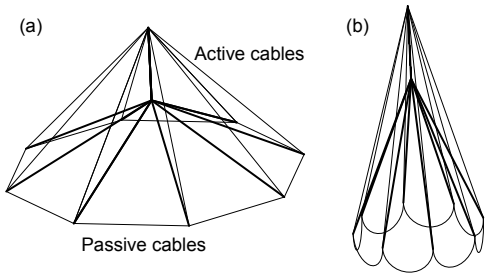

Fig. 1 Deployment of the cable-strut system
(a) Fully developed state; (b) Semi-foldable state

The deployment of a shelter based on CPs is achieved by tightening the inclined cables (Fig. 1). Thus, the inclined cables are active cables, whose length reduces as the shelter is deployed and increases as it is folded up. The passive cables of the shelter are the lower cables which are used to terminate deployment. In addition, more important function of passive cables is to increase the stiffness of the fully deployed structure. Another function of the active cables is to set up a state of self-stress in the fully deployed state, resulting in the pretension of all passive cables.

2.2 State of self-stress

In the fully deployed state of the shelter, there is only one state of self-stress and no inner mechanisms if no cable slackens. An equilibrium approach is used to find the prestressed stable form of the cable-strut structure. To set up a system of linear equilibrium equations, we used the axial force, denoted by q_{ij} in element ij, as a variable for each element. The equilibrium of Node 1 in the x, y, and z directions (Fig. 2) can respectively be written as

$$q_{12}\cos(\alpha/2)-q_{13}\cos(\alpha/2)=0, \tag{1}$$

$$q_{14}\cos\theta_2+q_{15}\cos\theta_1+q_{12}\sin(\alpha/2)+q_{13}\sin(\alpha/2)=0, \tag{2}$$

$$q_{14}\sin\theta_2+q_{15}\sin\theta_1=0, \tag{3}$$

where the angles α, θ_1, and θ_2 are given by

$$\alpha = \frac{2\pi}{N}, \tag{4}$$

$$\tan\theta_1 = \frac{2n}{l}, \tag{5}$$

$$\text{and } \tan\theta_2 = \frac{2(m+n)}{l}, \tag{6}$$

where N is the number of sides on the base polygon, m is the length of the vertical strut, n is the rise of the inner pyramid, and l is the span of the shelter.

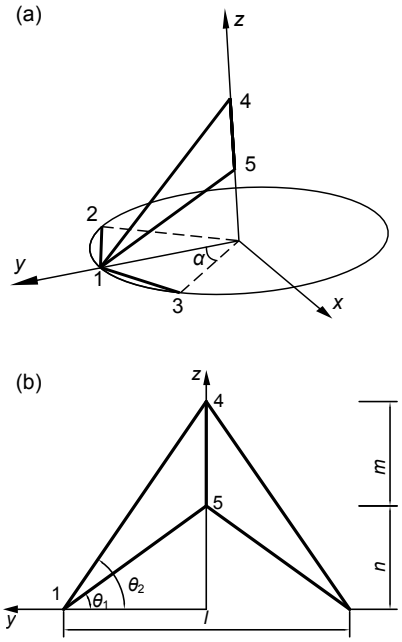

Fig. 2 Schematic diagram of the crystal-cell pyramid
(a) Elements meeting at node 1 of the structure; (b) Elevation drawing of the crystal-cell pyramid

From Eq. (1), we can obtain that

$$q_{12} = q_{13}. \tag{7}$$

This can also be obtained from the rotational symmetry of the structure.

Substituting Eq. (7) into Eqs. (2) and (3), we can obtain the tension relationship between the lower and inclined cables as

$$q_{14}\left(\cos\theta_2 - \frac{\sin\theta_2}{\tan\theta_1}\right) + 2q_{12}\sin\left(\frac{\alpha}{2}\right) = 0. \tag{8}$$

It is obvious that the axial force of the vertical strut is

$$q_{45} = -N \times q_{14}\sin\theta_2. \tag{9}$$

Thus, the self-stress state of the free-standing cable-strut is given by Eqs. (3), (8) and (9).

2.3 Minimum strut length design

Fig. 3 shows a CP cable-strut structure under an external load P. The weight of this structure includes the weight of bars and cables. However, the cable weight is negligible. Thus, the structure having the minimum weight also has the minimum total volume of bars. If all bars have the same section value, then the minimum length of bars leads to the minimum weight.

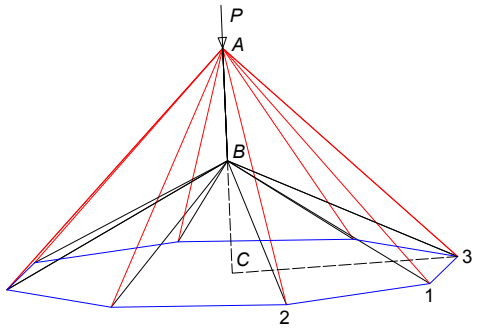

Fig. 3 Crystal-cell pyramid cable-strut structures under an external load

The global assumptions are: (1) The length of the lower and inclined cables is fixed and equal to l; (2) the number of base polygons of the two pyramids is N; and (3) the base polygon formed by the two pyramids is regular. Thus, the base of the CP cable-strut structure is an equilateral polygon (Fig. 4). Then the $\angle 1C2$ is an isosceles triangle and the corner angle is obtained from

$$\angle 1C2 = \frac{2\pi}{N}. \tag{10}$$

Then the length of $1C$ can be obtained from

$$1C = \frac{l/2}{\sin\dfrac{\angle 1C2}{2}} = \frac{l/2}{\sin\dfrac{\pi}{N}}. \tag{11}$$

The angle between the vertical strut and the inclined struts is assumed to be θ (Fig. 5). In $\Delta 1BC$, the length of the inclined strut $1B$ can be obtained from

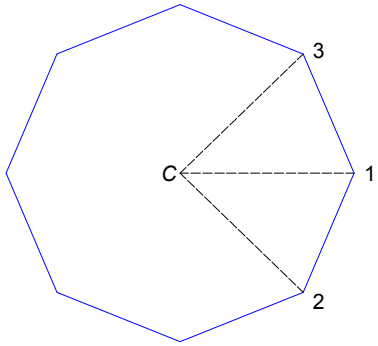

Fig. 4 Base of the crystal-cell pyramid cable-strut structure

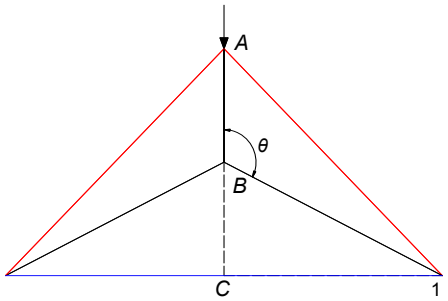

Fig. 5 Elevation drawing of the crystal-cell pyramid cable-strut structure

$$1B=\frac{1C}{\sin(\pi-\theta)}=\frac{1C}{\sin\theta}=\frac{l/2}{\sin\frac{\pi}{N}\sin\theta}. \tag{12}$$

In $\Delta 1AB$, it leads to

$$\frac{1A}{\sin\theta}=\frac{1B}{\sin\angle 1AB}. \tag{13}$$

Thus, the angle $\angle 1AB$ is

$$\angle 1AB=\arcsin\frac{1/2}{\sin(\pi/N)}. \tag{14}$$

Therefore, the length of $1A$, angle θ and $\angle 1AB$ are given, and the length of the vertical strut AB can be obtained from the following equation:

$$\frac{1A}{\sin\theta}=\frac{AB}{\sin\angle A1B}=\frac{AB}{\sin(\pi-\theta-\angle 1AB)}. \tag{15}$$

When the number of lower cables is three, the lengths of the vertical l_v and inclined struts l_i are given by

$$\begin{cases}\dfrac{l_v}{l}=\dfrac{\sqrt{6}}{3}+\dfrac{\sqrt{3}}{3\tan\theta},\\[2ex] \dfrac{l_i}{l}=\dfrac{1}{\sqrt{3}\sin\theta}.\end{cases} \tag{16}$$

Thus, the total length of the struts l_s is

$$\frac{l_s}{l}=\frac{l_v}{l}+\frac{3l_i}{l}=\frac{\sqrt{6}}{3}+\frac{\sqrt{3}}{3\tan\theta}+\frac{\sqrt{3}}{\sin\theta}. \tag{17}$$

Fig. 6 shows the relations between the length of the vertical struts, inclined struts and total struts, and the angle θ. The length of the vertical struts decreases with the increase in the angle θ. However, the length of the inclined struts increases with the angle θ. Thus, the total length of all the struts increases initially as the angle θ increases, then decreases. The total length of all the struts has a minimal value, and the corresponding angle θ can be obtained from

$$\frac{\mathrm{d}(l_s/l)}{\mathrm{d}\theta}=0. \tag{18}$$

Substituting Eq. (17) into Eq. (18) leads to

$$1+3\cos\theta=0. \tag{19}$$

Therefore, the corresponding angle θ to give the minimum length of total struts is 109°28′.

When the number of lower cables is four, the lengths of vertical and inclined struts are given as

$$\begin{cases}\dfrac{l_v}{l}=\dfrac{\sqrt{2}}{2}+\dfrac{\sqrt{2}}{2\tan\theta},\\[2ex] \dfrac{l_i}{l}=\dfrac{1}{\sqrt{2}\sin\theta}.\end{cases} \tag{20}$$

Thus, the total length of struts is

$$\frac{l_s}{l}=\frac{l_v}{l}+\frac{4l_i}{l}=\frac{\sqrt{2}}{2}+\frac{\sqrt{2}}{2\tan\theta}+\frac{2\sqrt{2}}{\sin\theta}. \tag{21}$$

The relations between the lengths of the vertical struts, inclined struts and total struts, and the angle θ are shown in Fig. 7. Structures with three or four lower cables show similar trends. The total length of

struts decreases initially and then increases with the increase in the angle θ.

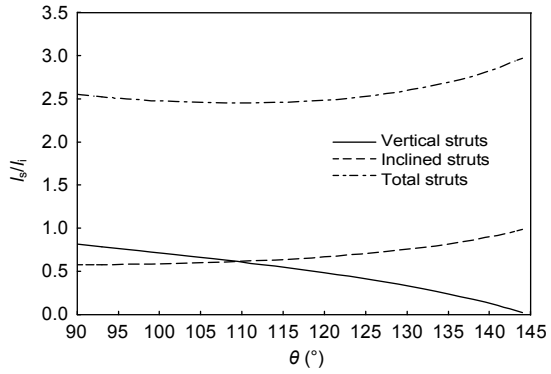

Fig. 6 Length of struts against angle θ when the number of lower cables is three

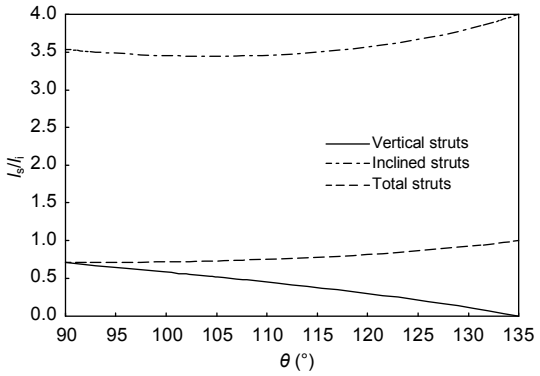

Fig. 7 Lengths of struts against angle θ when the number of lower cables is four

The total length of struts also has a minimal value, and the corresponding angle θ can be obtained by substituting Eq. (21) into Eq. (18):

$$1+4\cos\theta=0. \tag{22}$$

Thus, the angle θ corresponding to the minimum total length of struts of a shelter with four lower cables is 104°29′.

2.4 Maximum load design

In this section, the cross sections of vertical and inclined struts may be different. If the vertical strut is under an axial force load F, the axial stress is

$$\sigma_{\mathrm{v}}=-\frac{F}{A}, \tag{23}$$

where A is the area of cross sections. Then the axial stress of an inclined strut can be obtained from

$$\sigma_{\mathrm{i}}=-\frac{F}{NA\cos(\pi-\theta)}=\frac{F}{NA\cos\theta}. \tag{24}$$

If the total volume of struts for a shelter with a variable angle θ is a constant denoted as V, then the axial stresses of the vertical strut and inclined struts are given by

$$\begin{cases}\sigma_{\mathrm{v}}=-\dfrac{F}{V}l_{\mathrm{s}},\\ \sigma_{\mathrm{i}}=\dfrac{F}{V}\dfrac{l_{\mathrm{s}}}{N\cos\theta}.\end{cases} \tag{25}$$

The relative axial stress $\sigma/(F/V)$ of vertical and inclined struts with respect to the angle θ is shown in Fig. 8. The axial stress of vertical struts increases initially and then reduces as the angle θ increases. However, the axial stress of inclined struts increases as the angle θ increases. When the axial stress of the vertical struts reaches the minimal value, it is equal to the axial stress of the inclined struts. This, therefore, is the maximum load design of this model. The corresponding angle θ can be obtained from Eq. (18).

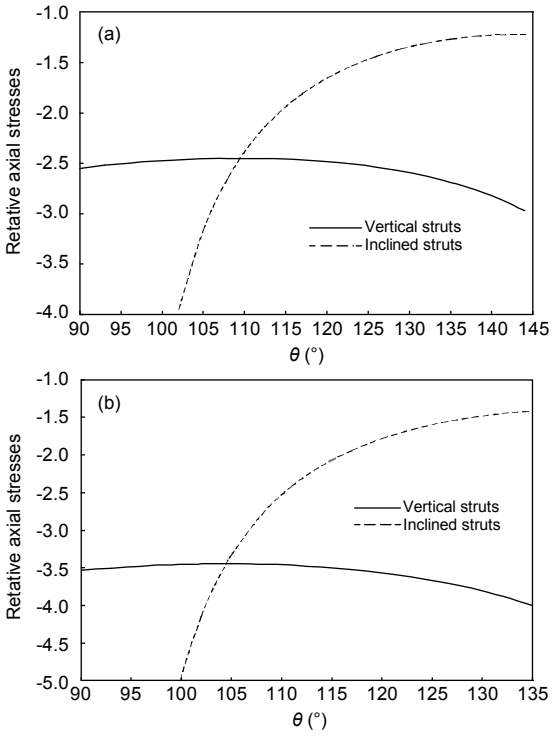

Fig. 8 Relative axial stress of struts against θ
(a) N=3; (b) N=4

3 Mechanical behavior of a cable-strut system

Structural behavior is one of the most important factors in determining the suitability of any proposed structural system for practical implementation. For the foldable shelter, the mechanical behavior in the deployed configuration is also very important.

3.1 Basic model

The design example used in this study is a CP cable-strut system with eight lower equatorial cables. The span and rise of the inner pyramid in the deployed configuration are 12 m and 4 m, respectively (making the rise-to-span ratio 1/3). The length of the vertical strut is 2 m. All nodes at the perimeter are assumed to be revolute joints. The principal members of the struts are made of steel with a Young's modulus of 210 GPa, and the cross-section is a steel pipe 80 mm in diameter with a 10 mm thick wall. Each of the cables has a diameter of 20 mm and a Young's modulus of 180 GPa. The inclined cables in the open configuration have an initial stress of 300 MPa. The initial stress of other elements can be obtained according to Section 2.2. The symmetrical load case g+s (dead load+snow load), called Load Case 1, was taken into account in all computations. The dead load g consists of a self-weight of 0.5 kN/m^2, including the contribution of all the struts and cables. The snow load is applied to the top surface of the structure in the vertical direction with a magnitude of 1.0 kN/m^2. A second load case (g+s/2), Load Case 2, is also considered in this study. This asymmetrical load case consists of the dead load g and the snow load s/2 distributed uniformly over a half span of the shell.

The finite element analysis software ANSYS was employed in all structural analyses that took into account the geometrical non-linearity. The struts were simulated by BEAM 188, and the joints were assumed to be pin-ended. The tension-only element LINK 10 was used to model the cables, which were pin-ended to the steel beams. SURFACE 154 was added between the inclined struts to impose the external dead load and snow load.

3.2 Results

The results of nodal displacements and stresses of inclined struts under the symmetrical load case are shown in Fig. 9. The maximum vertical nodal displacement of the shelter is −14.9 mm. The ratio of the maximal vertical displacement to the span of the structure is about 1/80. The maximum deflection is smaller than the maximum deflection limit of span/200. Thus, the structure satisfies the serviceability limit state condition. The mid-span displacement is −29.2 mm. The maximum stress of the inclined struts is 102 MPa, which is smaller than the design stress of the steel pipes. Therefore, the structure under Load Case 1 also meets the ultimate limit state condition.

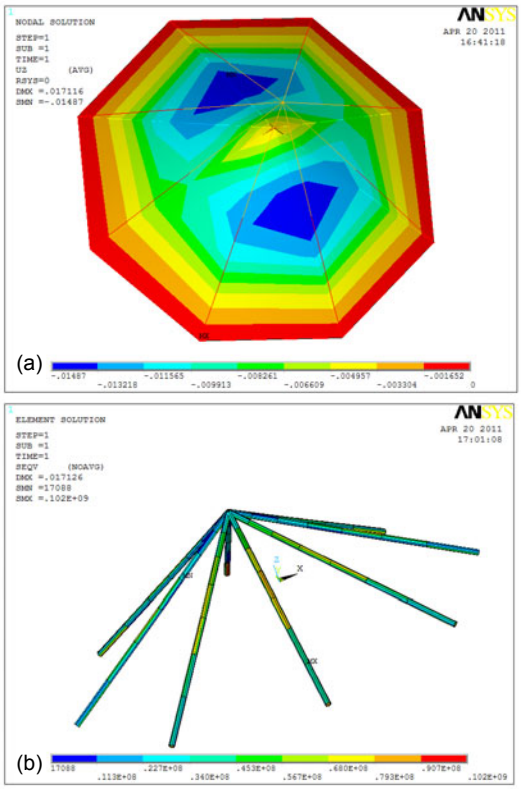

Fig. 9 Results for the shelter under Load Case 1
(a) Nodal displacement; (b) Element stress

Fig. 10 shows the nodal displacements and element stresses of struts under the asymmetrical load case. The deflection of the shelter is asymmetrical. The maximal nodal displacement is −13.2 mm and the maximal element stress is 95.3 MPa, which are smaller than the corresponding values of the structure under Load Case 1. Clearly, the shelter under Load Case 2 also meets the ultimate limit and the serviceability limit state conditions.

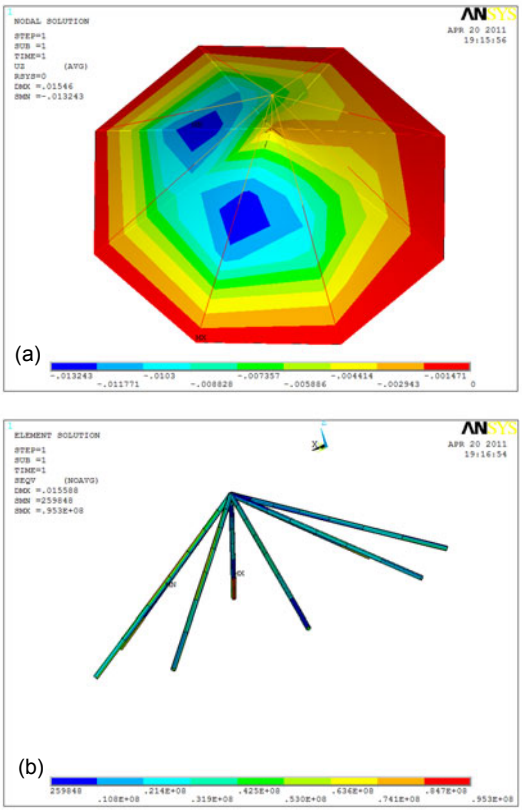

Fig. 10 Results for the shelter under Load Case 2
(a) Nodal displacement; (b) Element stress

4 Stability of cable-strut system

The static stability of cable-strut structures is also essential to the design of this type of structure.

4.1 Linear eigenvalue buckling analysis

The eigenvalue buckling analysis predicts the theoretical buckling capacity (the bifurcation load) of an ideal linear elastic structure. Although imperfections and material non-linearities often prevent most practical structures from achieving the theoretical elastic buckling capacity, eigenvalue buckling analysis is still a very useful tool to estimate the critical load and buckling modes for cable-strut structures. The first three critical loads for symmetrical loads are 9.76 kN/m^2, 9.77 kN/m^2, and 9.78 kN/m^2. For asymmetrical loads, the first three critical loads are 9.95 kN/m^2, 9.97 kN/m^2, and 10.02 kN/m^2. Some buckling modes of the structure under symmetrical and asymmetrical loads are shown in Figs. 11 and 12, respectively. The order of buckling modes for the two load cases is similar. Moreover, the buckling loads under Load Case 2 are slightly lower than those under Load Case 1. It is clear from the figures that the first two buckling modes are local buckling. From the third mode, the buckling modes are global. The shelter has high global stiffness in the open configuration.

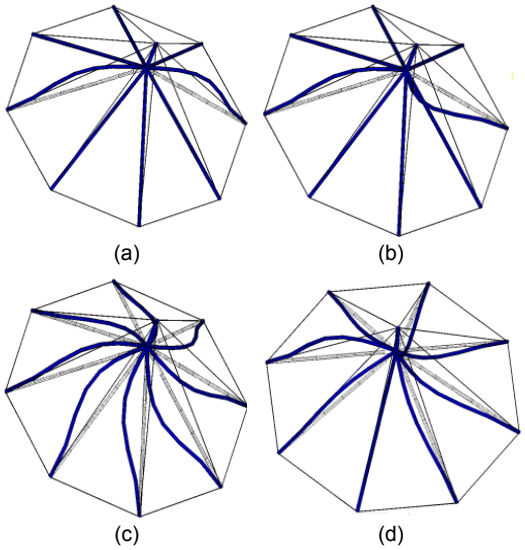

Fig. 11 Buckling modes of the shelter under Load Case 1
(a) First mode; (b) Second mode; (c) Third mode; (d) Fourth mode

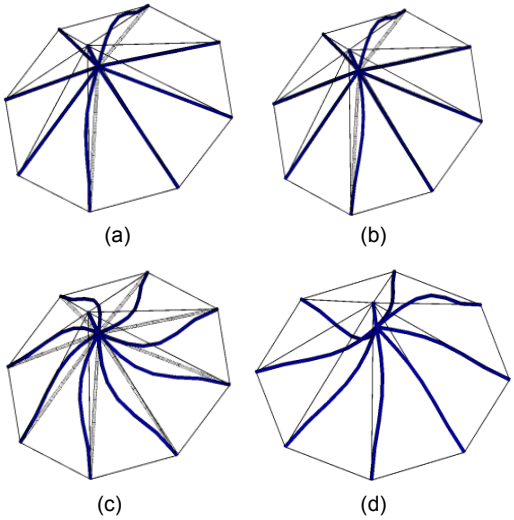

Fig. 12 Buckling modes of the shelter under Load Case 2
(a) First mode; (b) Second mode; (c) Third mode; (d) Fourth mode

4.2 Geometrical non-linear buckling analysis

This section focuses on the buckling analysis of the hybrid structure, considering the geometrical non-linearity. The Newton-Raphson method is used

to obtain the total load-displacement equilibrium path. Using this method, when the structure reaches the critical point, the tangent stiffness matrix of the structure becomes singular, causing severe convergence difficulties. A limit point is then reached along the load-displacement curve, and the buckling load is thereby obtained.

The relationship between the displacement at the node of interest (Node 5, Fig. 2) and the load for the two load cases is shown in Fig. 13. The load-displacement curves are similar for the two cases. The critical loads, 15.19 kN/m^2 and 17.42 kN/m^2, for the symmetrical and asymmetrical loads can be obtained from Fig. 13. Thus, the buckling load for asymmetrical loads is slightly higher than that for symmetrical loads. Thus, the asymmetrical distribution of load has only a limited effect on the buckling load obtained from the geometrical nonlinear analysis. However, the vertical displacement of Node 5 under Load Case 1 is larger than that under Load Case 2.

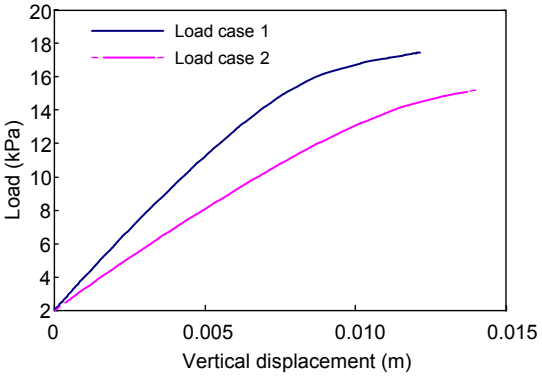

Fig. 13 Load-displacement curve for Node 5

4.3 Influence of imperfections

According to the European standard and Chinese code, geometrical imperfections should be taken into account in the non-linear analysis in order to model the structure in a more realistic way. Several methods are available for analyzing geometrical imperfections, including the random imperfection mode method and the consistent imperfection mode method.

In the consistent imperfection mode method, the imperfection distribution is assumed to be consistent with the first buckling mode of the structure, which is supposed to be close to the most undesired condition for the expected limit load.

According to the technical specification for space frame structures (JGJ7-2010), the maximum geometric imperfection caused by construction should be restricted within the limit of span/300. For the model in this study, the span is 12 m, and thus the maximum permitted geometric imperfection is 40 mm.

The buckling capacity of the structure decreases when the maximum nodal displacement (partly due to geometric imperfections) increases. The buckling loads for the imperfect shelter under the two load cases are 14.75 kN/m^2 and 17.35 kN/m^2. However, the effect of imperfections based on the first buckling mode on the shelter is minor.

5 Conclusions

In this paper, a foldable shelter system based on cable-strut structures was developed. The design and analysis of the shelter were discussed. Based on our results, the following conclusions can be drawn:

1. The total length of struts decreases initially then increases with the increase in the angle θ between the vertical strut and the inclined struts. Therefore, the total length of all struts has a minimal value.

2. When the axial stress of the vertical strut reaches the minimal value, it is equal to the axial stress of inclined struts. This is the maximum load design of this model.

3. The shelter in the deployed configuration under symmetrical and asymmetrical load cases satisfied the ultimate limit and the serviceability limit state conditions.

4. The buckling load for asymmetrical loads was slightly higher than that for symmetrical loads. An asymmetrical distribution of load has a limited effect on the buckling load obtained from the geometrical nonlinear analysis. Furthermore, the effect on the shelter of imperfections based on the first buckling mode is minor.

References

Cai, J.G., Feng, J., Wang, K., 2012. Deployment simulation of cable-strut structures considering cable sliding. *Science China: Technological Sciences*, **55**(12):3263-3269. [doi:10.1007/s11431-012-5034-z]

De Temmerman, I.N., Mollaert, M., Van Mele, T., De Laet, L.,

2007. Design and analysis of a foldable mobile shelter system. *International Journal of Space Structures*, **22**(3): 161-168. [doi:10.1260/026635107782218868]

Gioia, F., Dureisseix, D., Motro, R., Maurin, B., 2012. Design and analysis of a foldable/unfoldable corrugated architectural curved envelop. *Journal of Mechanical Design*, **134**(3):031003. [doi:10.1115/1.4005601]

Hangai, Y., Wu, M., 1999. Analytical method of structural behaviors of a hybrid structure consisting of cables and rigid structures. *Engineering Structures*, **21**(8):726-736. [doi:10.1016/S0141-0296(98)00027-3]

Hosozawa, O., Shimamura, K., Mizutani, T., 1999. The role of cables in large span spatial structures: introduction of recent space structures with cables in Japan. *Engineering Structures*, **21**(8):795-804. [doi:10.1016/S0141-0296(98)00032-7]

Juan, S.H., Mirats Tur, J.M., 2008. Tensegrity frameworks: static analysis review. *Mechanism and Machine Theory*, **43**(7):859-881. [doi:10.1016/j.mechmachtheory.2007.06.010]

Li, Y., Vu, K.K., Liew, J.Y.R., 2011. Deployable cable-chain structures: morphology, structural response and robustness study. *Journal of the International Association for Shell and Spatial Structures*, **52**(168):83-96.

Liew, J.Y.R., Tran, T.C., 2006. Novel deployable strut-tensioned membrane structures. *Journal of the International Association for Shell and Spatial Structures*, **47**: 17-29.

Liew, J.Y.R., Lee, B.H., Wang, B.B., 2003. Innovative use of star prism (SP) and di-pyramid (DP) for spatial structures. *Journal of Constructional Steel Research*, **59**(3):335-357. [doi:10.1016/S0143-974X(02)00037-8]

Liu, H.B., Chen, Z.H., Wang, X.D., 2011. Simulation of pre-stressing construction of suspen-dome considering sliding friction based large curvature assumption. *Advanced Science Letters*, **4**(8-10):2713-2718. [doi:10.1166/asl.2011.1716]

Luchsinger, R.H., Sydow, A., Crettol, R., 2011. Structural behavior of asymmetric spindle-shaped tensairity girders under bending loads. *Thin-Walled Structures*, **49**(9): 1045-1053. [doi:10.1016/j.tws.2011.03.012]

Mao, D.C., Luo, Y.Z., You, Z., 2007. A generalization of Kempe's linkages. *Journal of Zhejiang University-SCIENCE A*, 7(8):1365-1371. [doi:10.1631/jzus.2007.A1084]

Makowski, Z.S., 1981. Analysis, Design and Construction of Double-layer Grids. Applied Science Publishers Ltd., London.

Melin, N., 2004. Application of Bennett Mechanisms to Long-Span Shelters. University of Oxford.

Motro, R., 1992. Tensegrity systems: the state of the art. *International Journal of Space Structures*, **7**(2):75-83.

Motro, R., 2003. Tensegrity: Structural Systems for the Future. Kogan Page Science, London.

Quirant, J., Kazi-Aoual, M.N., Motro, R., 2003. Designing tensegrity systems: the case of a double layer grid. *Engineering Structures*, **25**(9):1121-1130. [doi:10.1016/S0141-0296(03)00021-X]

Rhode-Barbarigos, L., Bel Hadj Ali, N., Motro, R., Smith, I.F.C., 2012. Design aspects of a deployable tensegrity-hollow-rope footbridge. *International Journal of Space Structures*, **27**(2):81-96. [doi:10.1260/0266-3511.27.2-3.81]

Saitoh, M., Okada, A., 1999. The role of string in hybrid string structures. *Engineering Structures*, **21**(8):756-769. [doi:10.1016/S0141-0296(98)00029-7]

Seffen, K.A., 2012. Compliant shell mechanisms. *Philosophical Transactions of The Royal Society A Mathematical Physical and Engineering Sciences*, **370**:2010-2016. [doi:10.1098/rsta.2011.0347]

Vu, K.K., Liew, J.Y.R., Krishnapillai, A., 2005. Commutative algebra in structural analysis of deployable tension-strut structures. *Journal of the International Association for Shell and Spatial Structures*, **46**:173-178.

Vu, K.K., Liew, J.Y.R., Anandasivam, K., 2006a. Deployable tension-strut structures: from concept to implementation. *Journal of Constructional Steel Research*, **62**(3):195-209. [doi:10.1016/j.jcsr.2005.07.007]

Vu, K.K., Liew, J.Y.R., Anandasivam, K., 2006b. Deployable tension-strut structures: structural morphology study and alternative form creations. *International Journal of Space Structures*, **21**(3):149-164. [doi:10.1260/026635106779380494]

Wang, B.B., 1998. Cable-strut systems: part II—cable-strut. *Journal of Constructional Steel Research*, **45**(3):291-299. [doi:10.1016/S0143-974X(97)00076-X]

Wang, B.B., 2004. Free-standing Tension Structures: from Tensegrity Systems to Cable-Strut Systems. Spon Press, New York.

Wang, B.B., Li, Y.Y., 2003a. Novel cable-strut grids made of prisms: part I. basic theory and design. *Journal of International Association of Shell and Spatial Structures*, **44**:93-108.

Wang, B.B., Li, Y.Y., 2003b. Novel cable-strut grids made of prisms: part II. deployable and architectural studies. *Journal of International Association of Shell and Spatial Structures*, **44**:109-125.

Xue, W.C., Liu, S., 2009. Design optimization and experimental study on beam string structures. *Journal of Constructional Steel Research*, **65**(1):70-80. [doi:10.1016/j.jcsr.2008.08.009]